Communication: Broad manifold of excitonic states in light-harvesting complex 1 promotes efficient unidirectional energy transfer in vivo

Sara H. Sohail, Peter D. Dahlberg, Marco A. Allodi, Sara C. Massey, Po-Chieh Ting, Elizabeth C. Martin, C. Neil Hunter, and Gregory S. Engel

Citation: The Journal of Chemical Physics **147**, 131101 (2017);

View online: https://doi.org/10.1063/1.4999057

View Table of Contents: http://aip.scitation.org/toc/jcp/147/13

Published by the American Institute of Physics

Communication: Broad manifold of excitonic states in light-harvesting complex 1 promotes efficient unidirectional energy transfer *in vivo*

Sara H. Sohail,[1,a)] Peter D. Dahlberg,[2,a)] Marco A. Allodi,[1] Sara C. Massey,[1] Po-Chieh Ting,[1] Elizabeth C. Martin,[3] C. Neil Hunter,[3] and Gregory S. Engel[1,b)]

[1]*Department of Chemistry, Institute for Biophysical Dynamics, and The James Franck Institute, The University of Chicago, Chicago, Illinois 60637, USA*

[2]*Graduate Program in the Biophysical Sciences, Institute for Biophysical Dynamics, and The James Franck Institute, The University of Chicago, Chicago, Illinois 60637, USA*

[3]*Department of Molecular Biology and Biotechnology, University of Sheffield, Firth Court, Western Bank, Sheffield S10 2TN, United Kingdom*

(Received 4 August 2017; accepted 15 September 2017; published online 4 October 2017)

In photosynthetic organisms, the pigment-protein complexes that comprise the light-harvesting antenna exhibit complex electronic structures and ultrafast dynamics due to the coupling among the chromophores. Here, we present absorptive two-dimensional (2D) electronic spectra from living cultures of the purple bacterium, *Rhodobacter sphaeroides*, acquired using gradient assisted photon echo spectroscopy. Diagonal slices through the 2D lineshape of the LH1 stimulated emission/ground state bleach feature reveal a resolvable higher energy population within the B875 manifold. The waiting time evolution of diagonal, horizontal, and vertical slices through the 2D lineshape shows a sub-100 fs intra-complex relaxation as this higher energy population red shifts. The absorption (855 nm) of this higher lying sub-population of B875 before it has red shifted optimizes spectral overlap between the LH1 B875 band and the B850 band of LH2. Access to an energetically broad distribution of excitonic states within B875 offers a mechanism for efficient energy transfer from LH2 to LH1 during photosynthesis while limiting back transfer. Two-dimensional lineshapes reveal a rapid decay in the ground-state bleach/stimulated emission of B875. This signal, identified as a decrease in the dipole strength of a strong transition in LH1 on the red side of the B875 band, is assigned to the rapid localization of an initially delocalized exciton state, a dephasing process that frustrates back transfer from LH1 to LH2. *Published by AIP Publishing.* https://doi.org/10.1063/1.4999057

Photosynthetic light harvesting machinery has evolved highly efficient energy transfer processes to power an organism's metabolism using solar photons.[1–3] Light-harvesting complexes funnel excitations to the reaction center where charge separation is initiated; the dynamics of this photosynthetic excitonic energy transfer occur on the femtosecond to picosecond time scale.[4] Two-dimensional electronic spectroscopy (2DES) probes this energy transfer process using a sequence of ultrafast laser pulses.[5–9] 2DES correlates excitations at specific frequencies to the ground state bleach, stimulated emission, and excited state absorption signals they generate with femtosecond time resolution. The position, lineshape, and dynamics of 2DES spectral features are determined by the underlying electronic and vibrational structures of the system.[10–13]

Recent advances in GRadient Assisted Photon Echo Spectroscopy (GRAPES) have enabled 2DES spectra of highly scattering samples, including intact cells.[14,15] However, to date, only the measurement of the rephasing photon echo signal was feasible without alteration of the experimental geometry,[16] precluding direct acquisition of fully absorptive 2DES spectra, which offer the highest degree of spectral resolution. In complex systems, analysis of the fully absorptive 2DES spectra is critical to properly quantify and assign spectral dynamics and determine homogeneous and inhomogeneous contributions from a diverse ensemble.[17] Here, we present absorptive 2D spectra of the photosynthetic antenna complexes, light-harvesting complex 1 (LH1) and light-harvesting complex 2 (LH2), in living cells of the purple bacterium, *Rhodobacter* (*Rba.*) *sphaeroides.* We observe ultrafast relaxation of an inhomogeneous distribution of chromophores on a sub-100 fs time scale in wild-type (WT) cells, LH2-only cells, and LH1-only cells. In LH1-only cells, we also observe ultrafast intra-complex energy relaxation within a manifold of higher lying excitonic states. Acquisition of these spectra requires an experimental advance in the GRAPES methodology that enables the simultaneous acquisition of both the rephasing photon echo and nonrephasing free induction decay (FID) signals.

In WT *Rba. sphaeroides*, LH1, the core pigment-protein antenna complex, forms a dimeric complex around the reaction center, while LH2 is a peripheral pigment-protein antenna complex.[18] LH2 transfers energy to LH1 on a 5-7 ps time scale.[19,20] LH1 then transfers the excitation to the reaction center special pair on a 35 ps time scale.[21] LH2 contains

[a)]S. H. Sohail and P. D. Dahlberg contributed equally to this work.
[b)]Author to whom correspondence should be addressed: gsengel@uchicago.edu. Telephone: (773-834-0818).

B800 and B850 rings of bacteriochlorophyll *a* (BChl *a*).[22] The B850 ring consists of 18 strongly coupled BChl *a* molecules (~300 cm^{-1}), while the 9 BChl *a* in B800 are weakly coupled (~20 cm^{-1}).[21] Each LH1 dimer contains an S-shaped arrangement of strongly coupled (~300 cm^{-1}) BChl *a* molecules denoted as B875.[23,24]

2DES is a third-order nonlinear optical spectroscopy that provides information similar to transient absorption but with spectral resolution in both the excitation and detection axes. In a 2DES experiment, three incident electric fields generate an oscillating polarization that gives rise to a nonlinear signal in a unique phase-matched direction. The signal is heterodyne detected through interference with a reference pulse. A 2D scan of the time between pulses 1 and 2 (coherence time, τ) and the time between pulses 2 and 3 (waiting time, T) generates a 2D spectrum that correlates excitation energy with detection energy for each T.[25]

Interactions with pulses 1 and 3 generate oscillating polarizations that acquire phase with either the same or opposite sign, corresponding to nonrephasing and rephasing signals, respectively. These signals are generated in distinct phase-matched directions. The rephasing or nonrephasing spectra separately contain phase-twisted lineshapes with both absorptive and dispersive components (Fig. S2 of the supplementary material). Absorptive spectra are obtained by summing the nonrephasing and rephasing signals. Often, the time order of the first two pulses in a 2DES sequence is switched to enable the detection of both the rephasing and nonrephasing signals in a single phase-matched direction.[26] However, changing the pulse time-ordering requires two sequential measurements to calculate the fully absorptive 2DES spectra. Laser drift and sample degradation during the measurement may alter the conditions under which the rephasing or the nonrephasing signals are collected; thus, summation may not preserve the true dynamics or lineshape.

GRAPES spectra are acquired by focusing the pulses to lines, rather than points, and geometrically tilting the wavevector of pulse 1 relative to pulse 2, thereby spatially encoding the range of coherence time delays (Fig. 1).[27,28] As a result, all coherence times are encoded in each laser shot. Consequently, we collect a complete 2D spectrum with each laser shot, meaning we only need to scan over T, the time between pulses 2 and 3. The technical details of the GRAPES instrument are described in the supplementary material. In short, the temporal tilt imparted on pulse 1 relative to pulse 2 spatially encodes both positive and negative coherence times for each T; however, this tilt results in a gradient of waiting times for negative coherence times in a single laser shot, which restricts the acquisition of both the rephasing and nonrephasing signals.

Here, by integrating over 100 laser shots in each signal frame, we rapidly acquire (25 Hz) a series of GRAPES spectra while continuously scanning the waiting time delay stage (stage speed 25 fs/s) which yields 1 fs waiting time steps. We make use of our fine waiting time sampling to reconstruct a uniform waiting time for negative coherence times. By selecting signals generated from different frames (Fig. 1, top), we can linearly interpolate the signals to reconstruct negative coherence time data with a uniform waiting time

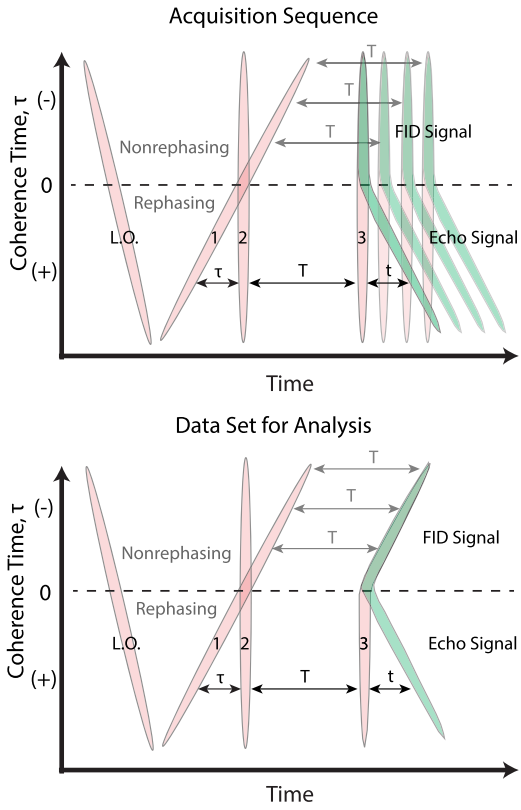

FIG. 1. (Top) The pulse sequence used in GRAPES that generates both third-order nonlinear rephasing photon echo and nonrephasing free induction decay (FID) signals in the same phase-matched direction. (Bottom) The finely sampled time delay between pulses 1 and 3 generates, for the purpose of analysis, a dataset that permits the nonrephasing signal at a constant waiting time (T) to be reconstructed from the raw data.

(Fig. 1, bottom). This interpolation rectifies the temporal gradient between pulses 1 and 3, which previously prohibited the measurement of nonrephasing signals from GRAPES without also changing the experimental geometry or the acquisition sequence. The interpolation is simplified by GRAPES data being acquired in the rotating frame, which eliminates fast oscillatory behavior.[27] In this way, we collect both the rephasing photon echo and the nonrephasing free induction decay signals in a single dataset.

We use the absorptive 2D spectra to probe ultrafast events in living *Rba. sphaeroides* cells, using WT, LH2-only, and LH1-only strains (Fig. 2). The growth and isolation protocols are detailed in the supplementary material. The 2DES data from the three cell types were phased to pump-probe spectra of membrane fragments (Fig. S2 of the supplementary material).[16,29] Both the WT and LH2-only spectra show diagonal excited state absorption (negative) and stimulated emission and ground state bleach (positive) features at 850 nm and 800 nm, corresponding to the B850 and B800 bands of LH2, respectively. Waiting time traces showing the dynamics of B850, B800, and energy transfer from B800 to B850 (Fig. S3 of the supplementary material) agree with prior measurements of LH2.[30] The spectra of LH1-only and WT cells show a diagonal peak around 870 nm corresponding to the B875 chromophores in LH1.[29]

The diagonal features in Fig. 2 all exhibit diagonal elongation at early waiting times, indicating inhomogeneous

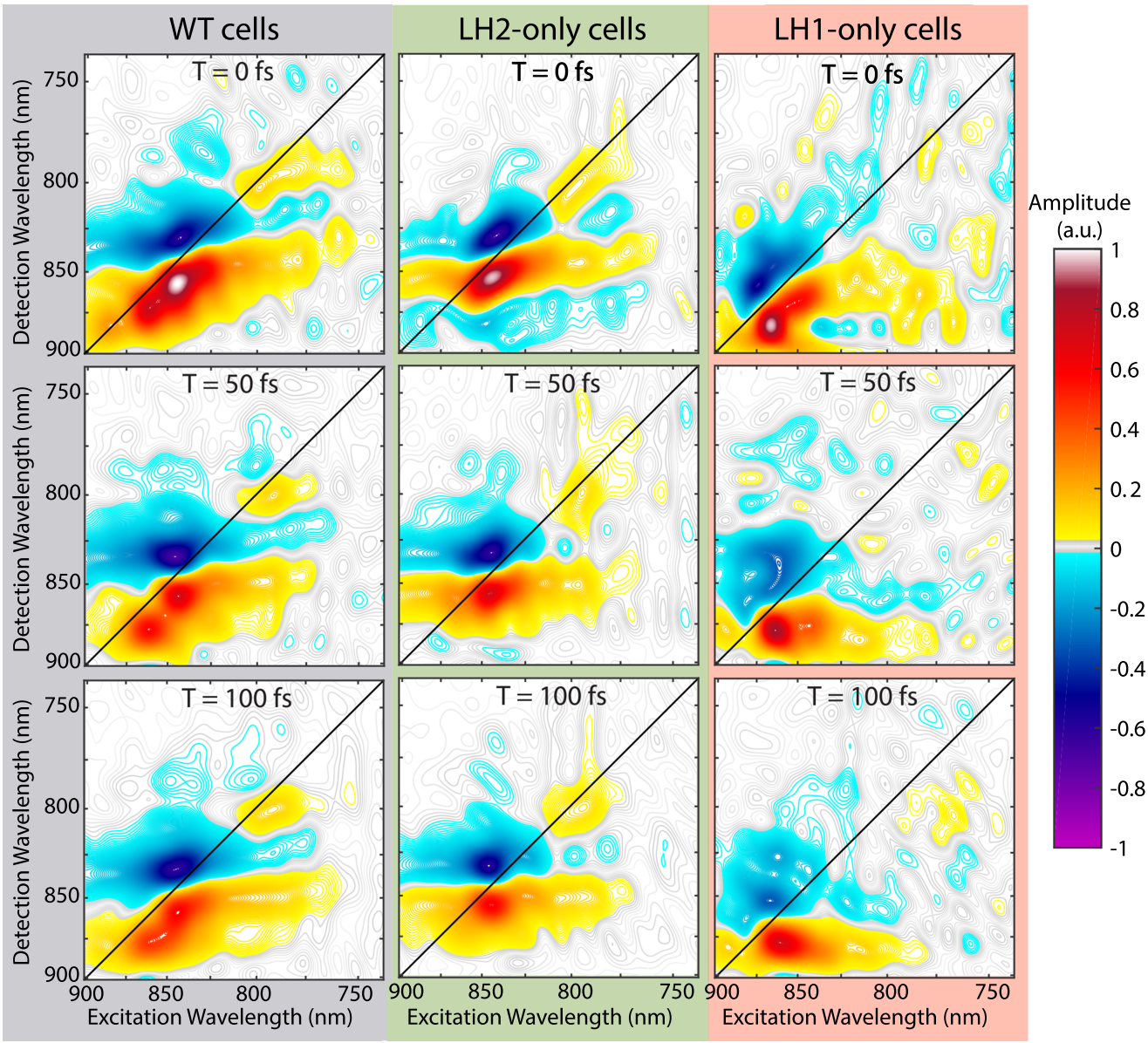

FIG. 2. Fully absorptive 2DES spectra for WT cells (left), LH2-only cells (center), and LH1-only cells (right); T = 0 fs (top), 50 fs (middle), and 100 fs (bottom). Spectral diffusion from the elongated, inhomogeneous lineshape to a round homogeneous lineshape can be seen as a function of T. The relaxation of the diagonal elongation of the spectral features indicates a loss of correlation between pump and probe energies as the system has had time to relax. The axis labels excitation and detection wavelength refers to the wavelengths resulting from a Fourier transform over the coherence time (τ) and the direct detection of the rephasing wavelength (λ_t), respectively. Axes are plotted as linear in frequency, but labeled by wavelength for ready comparison with linear spectra.

broadening of the B800, B850, and B875 bands. This elongation disappears by ~100 fs, reflecting relaxation within each spectral band. The degree of inhomogeneity in the 2DES absorptive spectra is quantified using the nodal line slope (NLS) analysis, which measures the tilt of the slope between the positive and negative features (Fig. S4 of the supplementary material).[10,31,32] The NLS analysis and NLS waiting time dynamics are described in the supplementary material.

Previous 2DES studies of *Rba. sphaeroides in vivo* only presented the rephasing spectra.[14,15] Here, we present 2D absorptive spectra that eliminate phase-twist in the lineshapes.[10] Access to the 2D absorptive lineshapes of light harvesting complexes *in vivo* makes characterization of finer spectral features, even at early waiting times, possible. Fitting every point in the LH1-only cells spectra to an independent monoexponential function, $A\exp(-T/\tau) + B$, with no constraints on amplitude or lifetime, shows that the decay lifetimes within B875 are non-uniform. The lifetimes from the monoexponential fits show that the red edge of B875, in both excitation and detection wavelengths, decays faster than the rest of the feature [Fig. 3(b)]. When analyzing slices through features in the 2D spectra [Figs. 3(c)–3(e)], the rapid decay on the red edge of B875 shown in Figs. 3(c)–3(e) shows a loss of intensity on the red edge of B875 or what could be a dynamic blue shift in the central wavelength of the ground state bleach/stimulated emission feature. The observed trend in the dynamics presented in Fig. 3(b) provides a clearer picture of the dynamics. The analysis of the decay constants across the 2D spectrum demonstrates a loss on the red edge of B875 which is consistent with ultrafast exciton localization resulting in a decrease in

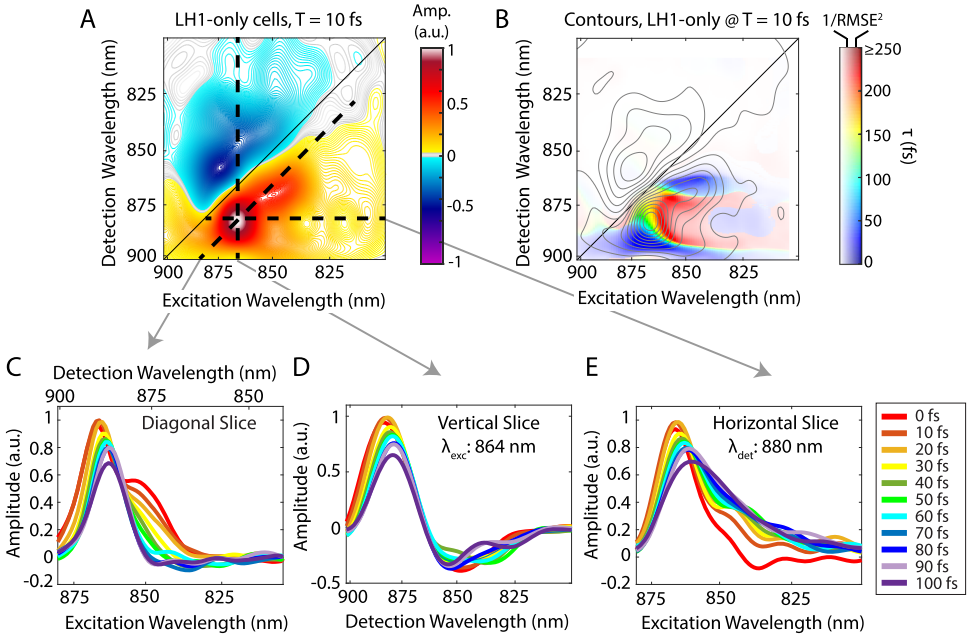

FIG. 3. (a) T = 10 fs spectrum of LH1-only cells. Black dashed lines indicate the locations of diagonal, vertical, and horizontal slices represented in (c)–(e), respectively. (b) The decay time at each point in the LH1-only cells spectra from a monoexponential fit ($A\exp(-T/\tau)+B$) at each point in the 2D spectrum. The color saturation is based on the root-mean-squared-error for the fit at each point. The gray contour depicts the 2DES spectrum at T = 10 fs. The (c) diagonal, (d) vertical, and (e) horizontal slices through the B875 stimulated emission/ground state bleach feature as a function of waiting time.

the transition dipole strength on the red side of the B875 band. This dynamic localization is similar to what has been reported for the B850 band of LH2.[33] However, we do not observe an analogous spectral pattern of decay times in the B850 feature of the LH2-only cells, though we see an ultrafast decay in the amplitude of the B850 feature (Fig. S5 of the supplementary material), consistent with B850 being more homogenous than B875 and previous reports on exciton localization in LH2.[14,33] The exciton localization on the red edge of B875 in LH1 would limit back transfer to LH2, but our WT data do not demonstratively illustrate how this rapid relaxation might impact transfer from LH1 to the reaction center. Though not explicitly mentioned, the decay on the red edge of the band appears in prior data from both 2DES rephasing spectra of LH1 membranes[29] and 3PEPS spectra of isolated LH1.[34] However, the 2DES spectra permit sufficiently increased resolution that we can now assign these dynamics more definitively.

The spectrum of decay times in Fig. 3(b) also shows the rapid decay of a higher energy B875 population at excitation wavelength = 850 nm and detection wavelength = 870 nm. The diagonal slices through B875 [Fig. 3(c)] reveal a bimodal distribution consisting of a lower energy population at excitation wavelength = 865 nm and detection wavelength = 880 nm and a higher energy population at excitation wavelength = 850 nm and detection wavelength = 870 nm. The higher energy population red shifts within 100 fs, as seen by the loss of the high energy distribution in the diagonal slices and the growth of intensity at excitation wavelength = 850 nm in the horizontal slices through detection wavelength = 880 nm [Fig. 3(e)]. Only the smaller, higher energy population within B875 is red shifting at early waiting times indicating an ultrafast intra-complex relaxation with a time constant <50 fs (Fig. S6 of the supplementary material). This dynamic red shift is also visible in the supplementary video of the *in vivo* 2DES spectra of the LH1-only mutant.

Relaxation within the LH1 manifold occurs on the same time scale as spectral diffusion, as indicated by the NLS analysis (Fig. S4 of the supplementary material). We suggest that the higher lying B875 population at early times (prior to the red shift) heavily contributes to the inhomogeneity measured using NLS. Previous work on LH1 using transient absorption spectroscopy showed a dynamic red shift of the B875 spectral feature on the 130-150 fs time scale, though these measurements were limited by an instrument response function of ~150 fs.[35] This dynamic red shift was more pronounced upon the blue side excitation of B875[35] and was attributed to downhill ultrafast excitonic relaxation in complementary Redfield theory calculations.[36] Our 2DES spectra indicate that only a portion of the inhomogeneous B875 feature is red shifting. Energy distributed through the broad manifold of LH1 states[29] is rapidly funneled into the lowest energy state, as exciton relaxation occurs.

A broad manifold of states with varied absorption/emission abilities within B875 offers an advantage for *Rba. sphaeroides* during light harvesting. The efficiency of light harvesting depends on how well excitation energy can hop between LH2 complexes and then to LH1 and on to the reaction center for charge separation. Prior to the dynamic red shift and exciton relaxation, higher lying populations observed in LH1 help maximize the spectral overlap with LH2, allowing for optimal energy transfer between the two antennae, while relaxation within LH1 minimizes back transfer into LH2. The spectral overlap that permits rapid transfer into the complex disappears as the higher-energy states relax, frustrating back transfer. The WT spectral dynamics are dominated by contributions from LH2 because the LH2 signal is stronger given our excitation spectrum and the high LH2:LH1 ratio in the WT strain (Fig. S1 of the supplementary material). Due to the separation of time scales between intra- and inter-complex dynamics,[37] we attribute the ultrafast dynamics observed in the LH1-only cells to the native behavior of this complex.

Our fully absorptive 2DES spectra of living *Rba. sphaeroides* cells reveal ultrafast exciton relaxation through

a manifold of higher lying excited states in LH1. The intra-complex relaxation in our spectra is supported by previous reports of a dynamic red shift in LH1, though the high resolution of our spectra at early waiting times indicates that only a resolvable sub-population within B875 is red shifting. This ultrafast relaxation and the rapid localization within LH1 indicate that the electronic structure of LH1 is effectively tuned for unidirectional energy transfer from LH2 to LH1. The ability to resolve ultrafast spectral dynamics within a broad manifold of excitonic states will enable the study of more complex energy transfer pathways in higher photosynthetic organisms.

See supplementary material for supporting figures, video of 2DES spectra of LH1-only mutants, analysis, growth protocols, and spectroscopic procedures.

The authors would like to thank MRSEC (No. DMR 14-20709), AFOSR (Grant No. FA9550-14-1-0367), the DoD Vannevar Bush Fellowship (Grant No. N00014-16-1-2513), the Camille and Henry Dreyfus Foundation, and the Sloan Foundation for supporting the work in this publication. S.H.S. and S.C.M. acknowledge support from DoD, Air Force Office of Scientific Research, National Defense Science and Engineering Graduate (NDSEG) Fellowship, 32 CFR 168a. P.D.D. acknowledges support from the NSF-GRFP program, and the National Institute of Biomedical Imaging and Bioengineering of the National Institutes of Health under Award No. T32-EB009412. M.A.A. acknowledges support from the Yen Fellowship at UChicago and from an Arnold O. Beckman Postdoctoral Fellowship from the Arnold and Mabel Beckman Foundation. C.N.H. and E.C.M. were supported by Grant No. BB/M000265/1 from the Biotechnology and Biological Sciences Research Council (UK) and an Advanced Award from the European Research Council (No. 338895). This research was also supported by the Photosynthetic Antenna Research Center (PARC), an Energy Frontier Research Center funded by the U.S. Department of Energy, Office of Science, Office of Basic Energy Sciences under Award No. DE-SC 0001035. That grant provided partial support for C.N.H.

[1] G. R. Fleming and R. van Grondelle, Curr. Opin. Struct. Biol. **7**, 738 (1997).
[2] R. E. Blankenship, *Molecular Mechanisms of Photosynthesis* (Blackwell Science, Oxford, Malden, MA, 2002).
[3] M. Sener, J. Strumpfer, J. Hsin, D. Chandler, S. Scheuring, C. N. Hunter, and K. Schulten, ChemPhysChem **12**, 518 (2011).
[4] H. van Amerongen, L. Valkunas, and R. van Grondelle, *Photosynthetic Excitons* (World Scientific, Singapore, River Edge, NJ, 2000).
[5] T. Brixner, J. Stenger, H. M. Vaswani, M. Cho, R. E. Blankenship, and G. R. Fleming, Nature **434**, 625 (2005).
[6] G. S. Schlau-Cohen, A. Ishizaki, and G. R. Fleming, Chem. Phys. **386**, 1 (2011).
[7] J. Dostal, T. Mancal, R. Augulis, F. Vacha, J. Psencik, and D. Zigmantas, J. Am. Chem. Soc. **134**, 11611 (2012).
[8] J. Dostal, J. Psencik, and D. Zigmantas, Nat. Chem. **8**, 705 (2016).
[9] F. D. Fuller, J. Pan, A. Gelzinis, V. Butkus, S. S. Senlik, D. E. Wilcox, C. F. Yocum, L. Valkunas, D. Abramavicius, and J. P. Ogilvie, Nat. Chem. **6**, 706 (2014).
[10] P. Hamm and M. T. Zanni, *Concepts and Methods of 2D Infrared Spectroscopy* (Cambridge University Press, Cambridge, New York, 2011).
[11] D. M. Jonas, Annu. Rev. Phys. Chem. **54**, 425 (2003).
[12] M. Cho, Chem. Rev. **108**, 1331 (2008).
[13] F. D. Fuller and J. P. Ogilvie, Annu. Rev. Phys. Chem. **66**(66), 667 (2015).
[14] P. D. Dahlberg, A. F. Fidler, J. R. Caram, P. D. Long, and G. S. Engel, J. Phys. Chem. Lett. **4**, 3636 (2013).
[15] P. D. Dahlberg, G. J. Norris, C. Wang, S. Viswanathan, V. P. Singh, and G. S. Engel, J. Chem. Phys. **143**, 101101 (2015).
[16] V. P. Singh, A. F. Fidler, B. S. Rolczynski, and G. S. Engel, J. Chem. Phys. **139**, 084201 (2013).
[17] A. Tokmakoff, J. Phys. Chem. A **104**, 4247 (2000).
[18] M. L. Cartron, J. D. Olsen, M. Sener, P. J. Jackson, A. A. Brindley, P. Qian, M. J. Dickman, G. J. Leggett, K. Schulten, and C. N. Hunter, Biochim. Biophys. Acta **1837**, 1769 (2014).
[19] P. D. Dahlberg, P.-C. Ting, S. C. Massey, M. A. Allodi, E. C. Martin, C. N. Hunter, and G. S. Engel, e-print arXiv:1706.08013 (2017).
[20] S. Hess, M. Chachisvilis, K. Timpmann, M. R. Jones, G. J. Fowler, C. N. Hunter, and V. Sundström, Proc. Natl. Acad. Sci. U. S. A. **92**, 12333 (1995).
[21] V. Sundström, T. Pullerits, and R. van Grondelle, J. Phys. Chem. B **103**, 2327 (1999).
[22] A. Freer, S. Prince, K. Sauer, M. Papiz, A. Hawthornthwaite-Lawless, G. McDermott, R. Cogdell, and N. W. Isaacs, Structure **4**, 449 (1996).
[23] P. Qian, M. Z. Papiz, P. J. Jackson, A. A. Brindley, I. W. Ng, J. D. Olsen, M. J. Dickman, P. A. Bullough, and C. N. Hunter, Biochemistry **52**, 7575 (2013).
[24] M. Sener, J. Hsin, L. G. Trabuco, E. Villa, P. Qian, C. N. Hunter, and K. Schulten, Chem. Phys. **357**, 188 (2009).
[25] J. D. Hybl, A. A. Ferro, and D. M. Jonas, J. Chem. Phys. **115**, 6606 (2001).
[26] M. L. Cowan, J. P. Ogilvie, and R. J. D. Miller, Chem. Phys. Lett. **386**, 184 (2004).
[27] E. Harel, A. F. Fidler, and G. S. Engel, J. Phys. Chem. A **115**, 3787 (2011).
[28] E. Harel, A. F. Fidler, and G. S. Engel, Proc. Natl. Acad. Sci. U. S. A. **107**, 16444 (2010).
[29] P. D. Dahlberg, P.-C. Ting, S. C. Massey, E. C. Martin, C. N. Hunter, and G. S. Engel, J. Phys. Chem. A **120**, 4124 (2016).
[30] V. Novoderezhkin, M. Wendling, and R. van Grondelle, J. Phys. Chem. B **107**, 11534 (2003).
[31] J. D. Eaves, J. J. Loparo, C. J. Fecko, S. T. Roberts, A. Tokmakoff, and P. L. Geissler, Proc. Natl. Acad. Sci. U. S. A. **102**, 13019 (2005).
[32] S. T. Roberts, J. J. Loparo, and A. Tokmakoff, J. Chem. Phys. **125**, 084502 (2006).
[33] L. D. Book, A. E. Ostafin, N. Ponomarenko, J. R. Norris, and N. F. Scherer, J. Phys. Chem. B **104**, 8295 (2000).
[34] R. Jimenez, F. van Mourik, J. Y. Yu, and G. R. Fleming, J. Phys. Chem. B **101**, 7350 (1997).
[35] R. Monshouwer, A. Baltuška, F. van Mourik, and R. van Grondelle, J. Phys. Chem. A **102**, 4360 (1998).
[36] R. van Grondelle and V. I. Novoderezhkin, Phys. Chem. Chem. Phys. **8**, 793 (2006).
[37] V. Nagarajan and W. W. Parson, Biochemistry **36**, 2300 (1997).